Synthesized design of a fuzzy logic controller for an underactuated unicycle

Article *in* Fuzzy Sets and Systems · November 2012

DOI: 10.1016/j.fss.2012.04.004

3 authors, including:

Jian-Xin Xu
National University of Singapore
233 PUBLICATIONS **6,351** CITATIONS

SEE PROFILE

Zhao-Qin Guo
Singapore Institute of Manufacturing Technology (SIMTech)
21 PUBLICATIONS **475** CITATIONS

SEE PROFILE

Design and Implementation of a Takagi–Sugeno-Type Fuzzy Logic Controller on a Two-Wheeled Mobile Robot

Jian-Xin Xu, *Fellow, IEEE*, Zhao-Qin Guo, and Tong Heng Lee

***Abstract*—This paper presents a novel implementation of a Takagi–Sugeno-type fuzzy logic controller (FLC) on a two-wheeled mobile robot (2WMR), which consists of two wheels in parallel and an inverse pendulum. The control objective of the 2WMR is to achieve position control of the wheels while keeping the pendulum around the upright position that is an unstable equilibrium. The novelties of this work lie in three aspects. First, the FLC is a synthesized design which utilizes both heuristic knowledge and model information of the 2WMR system. The FLC structure, including the fuzzy labels, membership functions, and inference, is chosen based on heuristic knowledge about the 2WMR. The output parameters of the FLC are determined by comparing the output of the FLC with that of a linear controller at certain operating points, which avoids the difficulty and tediousness in manual tuning. The linear controller is designed based on a linearized model of the 2WMR system. Second, the proposed FLC is a simple and realizable design for real implementation. Only two fuzzy labels are adopted for each fuzzy variable. Sixteen fuzzy rules are used with eight output parameters and four range parameters for the membership functions to be determined. Third, the proposed FLC is successfully implemented on a real-time 2WMR for regulation and setpoint control tasks. Satisfactory responses are achieved when the 2WMR travels not only on a flat surface but also on an inclined surface. Through comprehensive experiment-based investigations, the effectiveness of the proposed FLC is validated, and the FLC shows superior performance than the existing methods.**

***Index Terms*—Linear controller, parameter determination, steady state, Takagi–Sugeno (T–S) fuzzy logic controller (FLC), trajectory planning, two-wheeled mobile robot (2WMR), underactuated system.**

I. Introduction

In RECENT years, the control of a two-wheeled mobile robot (2WMR) or a two-wheeled inverted pendulum has attracted attention from both researchers and engineers [1]–[11]. However, most of the published works are based on theoretical analysis, and results are obtained by simulations; only few researchers have implemented their proposed control schemes on real-time platforms. The well-known commercial product two-wheeled SEGWAY is a popular personal transporter. For research and education purposes, prototypes and products of two-wheeled mobile vehicles or robots have been designed in universities and research institutes [3]–[11]. The 2WMR usually consists of two wheels in parallel and an inverse pendulum. The control objective of the 2WMR is to perform position or velocity control of the wheels while stabilizing the pendulum around the upright position that is an unstable equilibrium point. This type of systems that have numbers of actuators fewer than the degrees of freedom to be controlled is defined as underactuated systems.

Due to the difference in mechanical configuration, underactuated 2WMRs can be classified into a class without input coupling where the actuator is mounted on the wheel (class A) and a class with input coupling where the actuator is mounted on the pendulum or chassis (class B). Class A is more complex in mechanical construction but easier in controller design owing to the absence of input coupling between the wheel and the pendulum. In contrast, class B is easier in mechanical construction but more challenging in controller design due to the input coupling between the wheel and the pendulum. Since existing works mostly focus on studying control of underactuated systems without input coupling, this work is devoted to the development and control of an underactuated 2WMR with input coupling. When building the prototype of the 2WMR, the motor shaft coupler is fixed at the center of the wheels, and the motor housing is rigidly connected to the inverse pendulum; thus, the torque generated by the motor directly acts on both the wheels and the pendulum with the same size but opposite directions, which results in the input coupling of the 2WMR system.

The control of the 2WMR and similar underactuated systems is a rather challenging problem even if no uncertainties are considered existing in the systems; thus, the problem has attracted much attention from researchers whose interest is in the field of control theory. In plenty of theoretical works, stabilizing algorithms based on Lyapunov theory, passivity, feedback linearization, etc., are developed for underactuated systems [14]–[19]. The effectiveness of the proposed controllers is verified through simulations. However, these controllers may not function well on real-life systems. First, the controller design and stability proving are based on the accurate mathematical models without considering any uncertainties; however, uncertainties and model mismatches between nominal mathematical models and real-life plants are inevitable. Second, some of the control algorithms are too complicated to be implemented. By realizing the fact that uncertainties could affect system performance or

Manuscript received April 9, 2012; revised August 5, 2012; accepted November 13, 2012. Date of publication November 30, 2012; date of current version June 21, 2013.

The authors are with the Graduate School for Integrative Sciences and Engineering, National University of Singapore, Singapore 119077, and also with the Department of Electrical and Computer Engineering, National University of Singapore, Singapore 117576 (e-mail: elexujx@nus.edu.sg; guozhaoqin@gmail.com; eleleeth@nus.edu.sg).

Color versions of one or more of the figures in this paper are available online at http://ieeexplore.ieee.org.

Digital Object Identifier 10.1109/TIE.2012.2230600

even devastate system stability, researchers are motivated to explore robust control designs for underactuated systems with uncertainties [12], [13], [20]–[22].

Real-time control of 2WMRs and similar underactuated systems is presented in [3]–[13]. In [5]–[8], a full-state-feedback linear controller is employed. However, the robustness of the linear controller is limited. In [3] and [9], a novel adaptive output recurrent cerebellar model articulation controller is proposed, which is a model-free design. Functions are used to approximate the system model; thus, the designed control algorithm is complex in mathematics and not evident in physics idea. Furthermore, there are plenty of controller parameters to be determined. In [10] and [11], two-wheeled self-balancing vehicles are developed. The basic principle for riding the two-wheeled vehicle is that the traveler's body leads forward to make the wheels accelerate and leads backward to make the wheels slow down. Essentially, the mobility of the scooter is not autonomous because the traveler is involved in the control. In [12] and [13], a coupled sliding-mode control method is proposed and implemented on an underactuated Fukuda pendulum system. The convergence of the system states is guaranteed under the condition that the system stays on the sliding surface. However, the system transient responses are hardly predictable, particularly when the system is not on the sliding surface.

The fuzzy logic control approach has been widely used in robotic control and applications as it provides a user-friendly interface for controller design and the knowledge of the designers can be incorporated directly as a set of fuzzy rules. Fuzzy logic controller (FLC) design is, in general, model free, which is complementary to model-based control design. FLC offers a nonlinear controller with robustness for systems with parametric and functional uncertainties, as well as disturbances. With the flexibility of structure design and parameter selection in FLC design, FLC can be easily incorporated with other control methods, such as linear matrix inequality (LMI) [4] and sliding-mode control [23]. In [4], a fuzzy traveling and position control algorithm is proposed for a 2WMR without input coupling. The wheel position or position error is not used for computing the control input. The position control of the 2WMR is achieved through specifying a reference angle for the pendulum. The reference angle is the output of a fuzzy system, which has the inputs as the wheel position error and the wheel velocity. Based on human experience, 49 fuzzy rules are established to describe the relationship between the wheel states and the pendulum reference angle. For a 2WMR without input coupling, the pendulum equilibrium position is always the upright position, while for a 2WMR with input coupling, the equilibrium of the pendulum varies with respect to the slope angle of the traveling surface and the ground friction. During the traveling, the ground friction is unknown to the designer; thus, it is difficult to specify the value of the desired pendulum angle that could result in the desired motion of the wheels. As a result, the FLC proposed in [4] is limitedly applicable to the 2WMR without input coupling. In this work, to achieve the position control of the 2WMR, a Takagi–Sugeno (T–S)-type FLC using full-state feedback is proposed. All the available states, including the wheel position, the wheel velocity, the pendulum tilting angle, and the pendulum angle velocity, are used for feedback. The proposed FLC is applicable to a 2WMR with or without input coupling. There are four inputs to the FLC, and each of them is associated with two fuzzy labels, which yields, in total, 16 fuzzy rules in the FLC design.

A difficulty in FLC design is the lengthy tuning process for FLC parameters, which is usually trial and error in nature. There are two groups of controller parameters in the proposed FLC: the four range parameters for the fuzzy sets of four input variables and the eight output parameters for the output of the 16 rules, considering the symmetry between the fuzzy rules. The range parameters are chosen using heuristic knowledge such as physical boundaries of input variables. The eight FLC output parameters cannot be easily decided through empirical investigation, because they jointly determine the control effectiveness and any change of a single parameter would affect the overall FLC response. It is difficult to make clear the relations among the eight parameters because the underactuated 2WMR system shows complex behaviors. The limitation of heuristic knowledge motivates us to explore partially model-based design. Considering that the FLC is essentially a state feedback controller with varying feedback gains, we introduce a simple method by aligning the FLC output with a linear feedback control output at eight particular operating points of the 4-D state space, where each operating point represents a specific scenario with only one rule being activated while the remaining 15 rules are inhibited. As such, for each time, we can determine one FLC output parameter. The linear controller is designed based on a linearized model of the 2WMR, and the feedback gains are first obtained through a linear quadratic regulator (LQR) method by simulation and later manually tuned during the implementation, as in [5].

For implementing the FLC on the 2WMR, two practical issues are addressed. First, the 2WMR traveling on an inclined surface is considered, which was missed in [3]–[7] and [9]–[11]. It is found that the pendulum is no longer balanced at the upright position but a new equilibrium which is directly related with the slope angle of the inclined surface. Accordingly, the reference position for the pendulum tilting angle is adjusted to achieve a better performance. Furthermore, a steady-state error of the wheel position would exist when the FLC only is applied. To eliminate the steady-state error, a compensation term is included in the controller design. Second, undesired motions are observed in the real implementation, such as backward motion or stopping during the traveling. A novel reference trajectory is proposed for the wheels. The reference trajectory is updated in every sampling interval to achieve a smooth response.

The main contributions of this paper are as follows.

1) Development of an underactuated 2WMR prototype with input coupling is presented. An FLC is proposed for real-time control of the 2WMR. The designed FLC is also applicable to underactuated systems without input coupling, such as the 2WMR prototype built in [4]. Compared with the FLC designed in [4], the proposed FLC has fewer fuzzy rules and parameters to be determined, which implies a simpler design.
2) The proposed FLC is a synthesized design which utilizes both the human knowledge and the model information. The FLC structure and membership function are

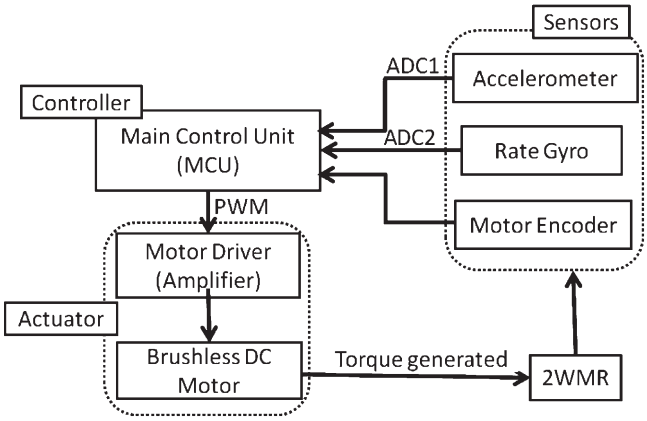

Fig. 1. System overview for the 2WMR.

determined using heuristic knowledge. The FLC output parameters are determined based on the output of a linear controller by specifying the 2WMR system states at 16 particular operating points in the 4-D state space, which avoids the difficulty in manual tuning. The new FLC outperforms a linear controller since it provides varying feedback gains that are desirable for real-time control of the 2WMR platform. Compared with the model-free designs in [3], [9], and [11], the FLC is simpler in mathematics; furthermore, it provides a user-friendly design interface. Thus, it is easy to understand.

3) The particular characteristics of the underactuated 2WMR system with input coupling are investigated, according to which references for both the wheel and the pendulum are designed to improve system performance. Regulation and setpoint control tasks are achieved when the 2WMR is placed not only on a flat surface but also on an inclined surface.

This paper is organized as follows. In Section II, the hardware configuration of the 2WMR is detailed. In Section III, the 2WMR dynamic model is given, and the control problem is formulated. In Section IV, the design procedure of the synthesized FLC is detailed. In Section V, the implementation of the FLC on a real platform is given. Conclusions are drawn in Section VI.

II. Hardware Description

Fig. 1 shows the overview of the hardware system. To measure the pendulum tilting angle and the pendulum angular velocity, an inertia measurement unit (IMU) combo board v1 (SparkFun Electronics) is used, which is equipped with an accelerometer (ADXL320) with a range of ± 5 g and a rate gyro (ADXRS613) capable of measuring up to $\pm 150^\circ/\mathrm{s}$. The IMU sensor produces analog output signals between 0 and 5 V; hence, analog-to-digital conversion is needed to generate digital signals that the main control unit (MCU) can process. In addition, the combo board also has a built-in low-pass filter for both the accelerometer and the rate gyro with cutoff frequencies of 500 and 40 Hz, respectively.

A brushless dc motor (Maxon Eci-40) is used as the only actuator, which generates the required torque to drive the wheels while balancing the pendulum. The brushless dc motor is controlled by a four-quadrant motor driver (Maxon DEC 70/10), which could also be regarded as an amplifier. The motor driver works under the mode of torque control, and the torque constant of the motor is 16.9 mN $\cdot$ m/A. A gearbox is mounted to the motor, which has a gear reduction ratio of $132:1$ with a gear efficiency of 80%. To obtain the position and velocity information of the wheels, a three-channel magnetic encoder is fixed on the motor. The encoder has a resolution of 500 counts per turn (CPT). By coupling the encoder and reduction gear with the motor, the resultant resolution is equivalent to 500×132 CPT.

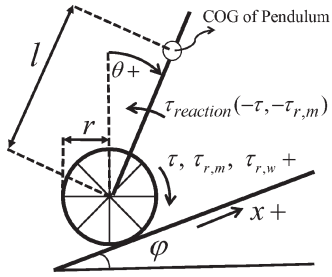

Fig. 2. Model of the 2WMR.

A Renesas microcontroller (SH7216) is used to process the data measured by the sensors, compute the control signal according to the designed control algorithm, and generate a pulsewidth-modulation signal for the motor driver. Renesas SH7216-FPU is a 32-b microcontroller capable of operating with a maximum frequency of 200 mHz and has a floating-point unit (FPU), 1 MB of ROM, and 128 kB of RAM. The MCU used meets the requirement for computation while maintaining a sufficiently high sampling frequency, which is 100 Hz in the implementation. The MCU can be programmed with C and C++ languages.

III. Modeling and Control Task

A. System Model

Fig. 2 shows the model of the 2WMR. The wheel motion is defined along the surface. The wheel displacement and velocity are denoted by x and $\dot{x}$, respectively, with rightward as the positive direction. θ is the tilting angle of the pendulum with the upright position as zero point and the clockwise rotation as positive direction. $\dot{\theta}$ is the angular velocity of the pendulum. φ is the slope angle of the inclined road; for traveling on a flat surface, $\varphi = 0$. $\tau_{r,w}$ is the rolling resistance from the traveling surface. τ is the torque generated by the motor and acting on the wheels with clockwise rotation as the positive direction, which is also the control input u to the system. Note that the motor driving the wheel is directly mounted on the pendulum; there is a reaction torque $-\tau$ applied to the pendulum. $\tau_{r,m}$ represents the resistance in the driving system, which also acts on both the wheel and the pendulum as $\tau_{r,m}$ and $-\tau_{r,m}$, respectively. Other system parameters are as follows: the mass of the wheels $m_w = 1.551$ kg, the mass of the pendulum $m_p = 1.6$ kg, the rotation inertia of the wheels $I_w = 0.005$ kg $\cdot$ m^2, the rotation inertia of the pendulum $I_p = 0.027$ kg $\cdot$ m^2, the radius of the wheel $r = 0.08$ m, the distance between the center of gravity (COG) of the pendulum and the center of the wheel $l = 0.13$ m, and the acceleration of gravity $g = 9.81$ m/s^2.

A Lagrangian mechanics method is used to derive the mathematical model of the 2WMR system, which leads to a second-order nonlinear model given by

$$a\ddot{x} + b\ddot{\theta} - m_p l \sin(\theta+\varphi)\dot{\theta}^2 + \sin\varphi(m_p+m_w)g = \frac{1}{r}(\tau + \tau_{r,m} - \tau_{r,w}) \quad (1)$$

$$b\ddot{x} + c\ddot{\theta} - m_p l g \sin\theta = -\tau - \tau_{r,m} \quad (2)$$

where $a = m_w + m_p + (I_w/r^2)$, $b = m_p l\cos(x_3+\varphi)$, and $c = I_p + m_p l^2$.

B. Control Objective and Trajectory Planning

The control objective of the 2WMR is to achieve setpoint control of the wheels while balancing the pendulum around an equilibrium ($\theta = \theta_e$ and $\dot{\theta} = 0$). Four state variables are defined to describe the 2WMR system, namely, the position and velocity of the wheels and the tilting angle and angular velocity of the pendulum, as $\mathbf{x} = [x_1, x_2, x_3, x_4]^{\mathrm{T}} = [x, \dot{x}, \theta, \dot{\theta}]^{\mathrm{T}}$. The reference signal for $\mathbf{x}$ is chosen as $\mathbf{r} = [x_r, v_r, \theta_r, 0]^{\mathrm{T}}$ with $\dot{x}_r = v_r$. Furthermore, we define the errors between the states $\mathbf{x}$ and their references $\mathbf{r}$ as $\mathbf{e} = [e_1, e_2, e_3, e_4]^{\mathrm{T}} = \mathbf{x} - \mathbf{r} = [x_1 - x_r, x_2 - v_r, x_3 - \theta_r, x_4]^{\mathrm{T}}$. Now, the control objective is to ensure the convergence of $\mathbf{e}$.

For the classical setpoint control task, a step signal is used as the reference. However, in real implementation, using a step function as the desired trajectory for the 2WMR would generate a large initial control signal due to the large initial position error, which yields a strong impact to the 2WMR and leads to unstable motion. To avoid the undesired impact, we convert the setpoint control task into a trajectory tracking task. High-order polynomials are sometimes used for computing a smooth trajectory [8]; however, in this work, we simply use a linear segment and two parabolic blends to construct a smooth trajectory for the 2WMR, which also yields a smooth reference signal for the wheel velocity. The reference inputs are computed by the following equations and shown in Fig. 3:

$$v_r(t) = \begin{cases} \frac{v_m}{t_1}t, & 0 < t < t_1 \\ v_m, & t_1 \le t \le t_2 \\ v_m - \frac{v_m}{t_3 - t_2}(t - t_2), & t_2 \le t \le t_3 \\ 0, & t_3 \le t \le t_s \end{cases} \quad (3)$$

$$x_r(t + T_s) = \begin{cases} x_r(t) + v_r T_s, & \text{if } x_r(t) < x_d \\ x_d, & \text{if } x_r(t) \ge x_d \end{cases} \quad (4)$$

where x_d is the desired setpoint and T_s is the sampling time.

The planned reference signals for the wheel position and velocity yield zero initial position and velocity errors, which are desirable for control of the 2WMR. According to Fig. 3, the 2WMR is supposed to move forward consistently and reach the setpoint $x_d = 1.5$ m around $t = t_3 = 16$ s.

IV. FLC Design

In this work, we adopt a T–S-type FLC for simplicity of the controller structure and easiness for the FLC parameter tuning. With full-state feedback, we have four inputs to the FLC. For each input, we use two fuzzy labels, namely, positive (P) and negative (N), for fuzzification. Therefore, there are, in total, $2^4 = 16$ fuzzy rules.

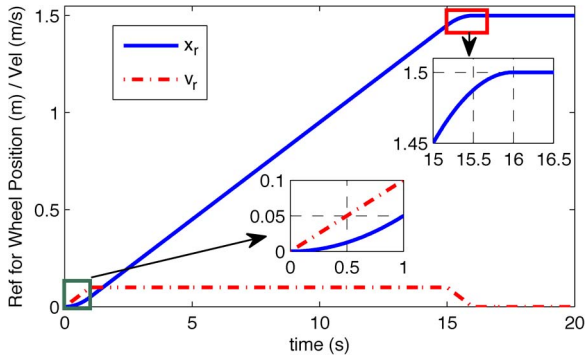

Fig. 3. Reference signals for the wheel velocity and position as described in (3) and (4) with $t_1 = 1$ s, $t_2 = 15$ s, $t_3 = 16$ s, $t_s = 20$ s, $v_m = 0.1$ m/s, and $x_d = 1.5$ m.

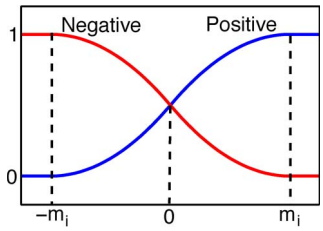

Fig. 4. Membership function used for FLC. The range of inputs is specified by an interval $[-m_i, m_i]$, $i = 1, 2, 3, 4$. Two fuzzy sets, denoted by P and N, are described by their membership functions, respectively. The membership function of P is a smooth curve described by a function as (5). The membership function of N is the complementary to that of P.

A. Structure of FLC

The four error states (e_1, e_2, e_3, and e_4) are the inputs to the FLC. Each of the four input variables is associated with two fuzzy sets P and N, respectively, and the degree to which set they belong to is determined by the membership function shown in Fig. 4.

A built-in membership function in the Matlab toolbox, named as the S-shaped membership function, is used to represent fuzzy set P and given as follows:

$$\mu_P(e_i) = \begin{cases} 0 & (e_i < -m_i) \\ 2\left(\frac{e_i + m_i}{2m_i}\right)^2 & (-m_i \le e_i \le 0) \\ 1 - 2\left(\frac{m_i - e_i}{2m_i}\right)^2 & (0 \le e_i \le m_i) \\ 1 & (e_i > m_i) \end{cases} \quad (5)$$

where μ_P is the matching degree to fuzzy set P. The matching degree to fuzzy set N, denoted as μ_N, is complementary to μ_P, i.e., $\mu_N = 1 - \mu_P$. Fuzzy set N is represented by another built-in membership function in the Matlab toolbox, named as the Z-shaped membership function, which is complementary to the S-shaped membership function.

There are three reasons to employ the Z- and S-shaped membership functions. First, the Z- and S-shaped membership functions are appropriate to represent the concepts of positive and negative. Second, the Z- and S-shaped membership functions

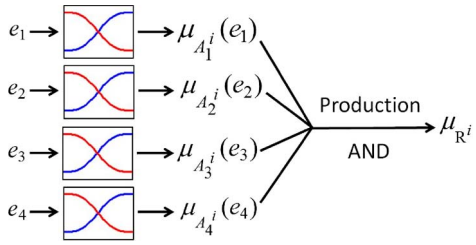

Fig. 5. T–S-type fuzzy inference for the ith rule ($i = 1-16$). Each input e_j ($j = 1-4$) yields two membership values $\mu_N(e_j)$ and $\mu_P(e_j)$. For individual fuzzy rules, A_j^i is specified as either P or N; accordingly, the value of $\mu_{A_j^i}(e_j)$ used for the calculation of μ_{R^i} is either $\mu_P(e_j)$ or $\mu_N(e_j)$. The AND logic operator in the antecedent part is chosen to be the production of four fuzzy membership values.

are second-order polynomials, which are suitable for the implementation of the FLC because of their easiness in computing. Third, the FLC using the S- and Z-shaped membership functions provides varying feedback gains that are desirable for control of the 2WMR. The third point will be explained later.

The range parameters (m_1, m_2, m_3, and m_4) are determined by taking the physical constraints of the 2WMR system into consideration. m_1 specifies the range of e_1, the tracking error of the wheel position. Considering that the radius of the wheel is 0.08 m, we assume that the maximum allowable tracking error of the wheel position is around the wheel circumference of 0.5 m; thus, m_1 is chosen to be 0.5 m. m_2 specifies the range of e_2, the tracking error of the wheel speed. Through experimental investigation, we found that the maximum wheel speed is around 0.35 m/s under the capacity of the dc motor used; hence, m_2 is chosen to be 0.35 m/s. m_3 specifies the range of the pendulum angular displacement. We consider that the pendulum moves within a safe range around the balanced position and choose $m_3 = \pi/6$ rad, i.e., 30°. m_4 specifies the range of the pendulum angular velocity and is chosen to be 0.2 rad/s, i.e., 11.5°/s.

The structure of the FLC is T–S type, which consists of rules of the following form:

$$R^i: \text{ If } \left(e_1 \text{ is } A_1^i\right) \text{ AND } \left(e_2 \text{ is } A_2^i\right) \text{ AND } \left(e_3 \text{ is } A_3^i\right) \text{ AND } \left(e_4 \text{ is } A_4^i\right), \text{THEN } (u_i = \tau_i)$$

where A_1^i, A_2^i, A_3^i, and $A_4^i \in \{P, N\}$ are the fuzzy sets or fuzzy labels, u_i is the rule output, and τ_i is a constant representing the desired control torque. Each fuzzy rule describes a specific relationship between the fuzzy inputs and output.

Each rule contributes to the final FLC output according to matching for the IF part of the fuzzy rule. The T–S-type fuzzy inference takes a weighted average of the individual outputs for each rule. The output τ_i ($i = 1-16$) for each rule is weighted by the firing strength μ_{R^i}, which is calculated as shown in Fig. 5.

Table I shows the 16 rules of the FLC for the 2WMR system. According to the table, the first IF–THEN rule can be expressed as

$$R^1: \text{ If } (e_1 \text{ is P}) \text{ AND } (e_2 \text{ is P}) \text{ AND } (e_3 \text{ is P}) \text{ AND } (e_4 \text{ is P}), \text{THEN } (u_i = \tau_i)$$

TABLE I
FUZZY RULES

Rule	$e_1(x-x_r)$	$e_2(\dot{x}-v_r)$	$e_3(\theta-\theta_r)$	$e_4(\dot{\theta})$	*Torque*
1	P	P	P	P	$\tau_1 = n_1$
2	P	N	P	P	$\tau_2 = n_2$
3	N	P	P	P	$\tau_3 = n_3$
4	N	N	P	P	$\tau_4 = n_4$
5	P	P	P	N	$\tau_5 = n_5$
6	P	N	P	N	$\tau_6 = n_6$
7	N	P	P	N	$\tau_7 = n_7$
8	N	N	P	N	$\tau_8 = n_8$
9	P	P	N	P	$\tau_9 = -n_8$
10	P	N	N	P	$\tau_{10} = -n_7$
11	N	P	N	P	$\tau_{11} = -n_6$
12	N	N	N	P	$\tau_{12} = -n_5$
13	P	P	N	N	$\tau_{13} = -n_4$
14	P	N	N	N	$\tau_{14} = -n_3$
15	N	P	N	N	$\tau_{15} = -n_2$
16	N	N	N	N	$\tau_{16} = -n_1$

and the firing strength for the first rule is

$$\mu_{R^1} = \mu_P(e_1)\mu_P(e_2)\mu_P(e_3)\mu_P(e_4).$$

The final output of the fuzzy controller is calculated by aggregating all 16 rules in the weighted form

$$u_{\text{flc}} = \frac{\sum_{i=1}^{16} \mu_{R^i}\tau_i}{\sum_{i=1}^{16} \mu_{R^i}}.$$

Due to the symmetry in fuzzy rule design, we have $\sum_{i=1}^{16} \mu_{R^i} = 1$, which yields

$$u_{\text{flc}} = \sum_{i=1}^{16} \mu_{R^i}\tau_i. \tag{6}$$

B. FLC Output Parameter Tuning

The tuning of the FLC output parameters is a critical issue as it directly determines the control signal. First, note the skew symmetry between the ith rule and the $(17-i)$th rule ($i = 1-8$) where the input variables have opposite fuzzy labels P and N; we have the output skew symmetry where the two rules give the same control amplitude n_i but opposite directions. Therefore, there are eight output parameters in total to be determined.

Essentially, the FLC could be regarded as a feedback controller with varying feedback gains

$$u_{\text{flc}} = -\mathbf{k}(\mathbf{e})^{\text{T}}\mathbf{e}. \tag{7}$$

To stabilize the 2WMR system, feedback control should be taken appropriately for all states. A simple linear feedback controller can help to reveal how a feedback controller works, which inspires us to tune the eight output parameters (n_1-n_8) using the knowledge of a linear feedback controller. The linear controller

$$\kappa = -\mathbf{k}^{\text{T}}\mathbf{e} \tag{8}$$

where $\mathbf{k} = [k_1, k_2, k_3, k_4]^{\text{T}}$, is designed based on a linearized dynamic model at the desired equilibrium point, and the LQR method is applied to obtain the feedback gains (refer to the Appendix).

The FLC output parameters are determined in the following manner. At first, let one rule be fully activated and the other 15 rules be inhibited by setting the four input variables at the limits of their ranges ($\pm m_i$). For instance, for R^1 which corresponds to $e_1 = \mathrm{P}$, $e_2 = \mathrm{P}$, $e_3 = \mathrm{P}$, and $e_4 = \mathrm{P}$, we choose $e_i = m_i,\ i = 1, 2, 3, 4$. Then, we can compare the output of the first fuzzy rule τ_1 with the output of the linear controller (8) with the same values of the four error quantities. In such circumstances, the value of the linear controller output given by (8) is equal to the first FLC rule output, i.e., $\tau_1 = n_1 = -k_1 m_1 - k_2 m_2 - k_3 m_3 - k_4 m_4$. In this way, we can determine all eight FLC output parameters n_i, $i = 1, \ldots, 8$.

Remark 1: There is a lack of systematic parameter design for FLC in general. Trial-and-error design is time consuming due to the high dimension of the parametric space and often yields poor performance. It would be even more difficult to determine the FLC output parameters in this work because the 2WMR system is an underactuated and highly nonlinear system, which shows complex behaviors, particularly the motions of the wheels. For instance, let the 2WMR be initially balanced at the origin, and a setpoint control task with $x_d > 0$ is assigned, i.e., the robot is supposed to move forward. From human knowledge, a positive torque should be applied to drive the wheels to move forward. However, through investigations, we found that, to achieve a stable response, a negative torque should be applied at first, which makes the wheels move backward and the pendulum tilt rightward a bit. After that, the wheels start to move forward. In fact, this is the typical control behavior of non-minimum-phase systems, and according to our theoretical analysis in [24], the underactuated 2WMR has unstable internal dynamics. Considering the 2WMR complex behaviors, in this work, to determine the FLC output parameters, we utilize both the system model information and the knowledge of a linear feedback controller. The resulting FLC is able to produce a control signal profile that tallies with the desired one for non-minimum-phase systems.

Remark 2: For implementation, the parameter tuning is inevitable due to the difference between simulation and experiment. In this work, we do not need to tune the 16 FLC output parameters directly. Instead, we tune the four feedback gains for the linear controller, according to which the FLC output parameters are computed. Thus, the tuning of the FLC output parameters in this work is much simpler than that in general FLC designs.

C. Steady-State Analysis

When the system enters steady state, i.e., the 2WMR stops at the desired position, we have $\ddot{x} = 0$, $\ddot{\theta} = 0$, $\dot{x} = 0$, $\dot{\theta} = 0$, $\tau_{r,m} = 0$, and $\tau_{r,w} = 0$. The system dynamic equations (1) and (2) become

$$\sin\varphi(m_p + m_w)g = \frac{1}{r}\tau \tag{9}$$

$$-m_p l g \sin\theta_e = -\tau. \tag{10}$$

From the above equations, we have

$$\theta_e = \arcsin\frac{r\sin\varphi(m_p + m_w)}{m_p l}. \tag{11}$$

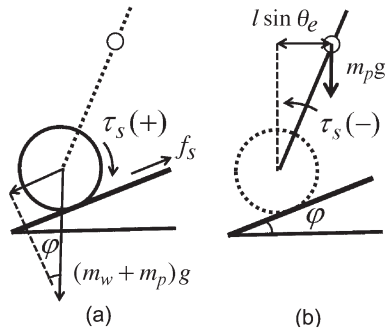

Fig. 6. Free-body diagrams of the 2WMR which is balanced on an inclined surface.

Remark 3: When the 2WMR travels on a flat surface, i.e., $\varphi = 0$, we have $\theta_e = 0$. The desired balance position of the pendulum is the upright position. When the 2WMR travels on an inclined surface, the pendulum equilibrium position θ_e depends on the size of the slope angle φ and is irrelevant to control input and control tasks.

Denoting τ_s as the torque needed in steady state, from (9), we have

$$\tau_s = r\sin\varphi(m_p + m_w)g. \tag{12}$$

The free-body diagrams of the wheel and the pendulum when the 2WMR is balanced on an inclined surface with $\varphi > 0$ are shown in Fig. 6(a) and (b), respectively.

In Fig. 6(a), f_s denotes the ground static friction. The force equation along the inclined surface is obtained as $f_s - (m_w + m_p)g\sin\varphi = 0$, while the torque equation of the wheel is $\tau_s - r f_s = 0$; thus, $\tau_s = r(m_w + m_p)g\sin\varphi$, which is consistent with the result in (12). Essentially, the torque τ_s is provided to overcome the effect of gravity and stabilize the wheel on the inclined surface. Meanwhile, the reaction torque $-\tau_s$ acts on the pendulum. From Fig. 6(b), we have the torque equation as $-\tau_s + m_p g l\sin\theta_e = 0$. The pendulum tilts rightward from the upright position and is balanced at $\theta = \theta_e$ such that the torque that resulted from the gravity of the pendulum is equal to the reaction torque $-\tau_s$ but with an opposite direction.

Define the steady-state error vector as $\mathbf{e}_s = [e_{1,s}, e_{2,s}, e_{3,s}, e_{4,s}]^{\mathrm{T}}$; to make $e_{3,s} = 0$, it is reasonable to choose the reference position for the pendulum tilting angle as $\theta_r = \theta_e$. At steady state, we have $(e_{2,s}, e_{3,s}, e_{4,s}) = (0, 0, 0)$, which yields $[\mu_P(e_{i,s}), \mu_N(e_{i,s})] = [0.5, 0.5],\ i = 2, 3, 4$. It follows that

$$\mu_{R^i} = \begin{cases} \mu_P(e_1)\cdot 0.5^3, & \text{for } i = 1, 2, 5, 6, 9, 10, 13, 14 \\ \mu_N(e_1)\cdot 0.5^3, & \text{for } i = 3, 4, 7, 8, 11, 12, 15, 16. \end{cases}$$

At steady state, the FLC in (6) becomes

$$u_{\mathrm{flc},s} = 0.125\left[\mu_P(e_{1,s}) - \mu_N(e_{1,s})\right]\sum_{i=1}^{8} n_i. \tag{13}$$

When applying the FLC designed in (6) to the 2WMR which travels on an inclined surface, at steady state, we have $u_{\mathrm{flc},s} = \tau_s$. From (13), we have $\mu_P(e_{1,s}) - \mu_N(e_{1,s}) \neq 0$ since $\tau_s \neq 0$. From the membership function in (5), we can conclude that $e_{1,s} \neq 0$, i.e., there is a steady-state error in the response of the wheel position.

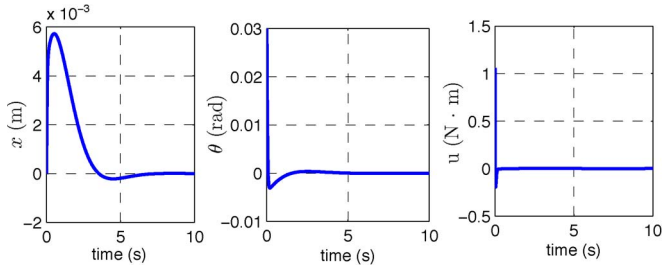

Fig. 7. Simulation results for the regulation task: Time responses of x, θ, and u under the linear controller. The nominal model of the 2WMR [(1) and (2)] is used for the simulation, and the system is considered without any uncertainties.

In this work, to achieve a satisfactory response with zero steady-state error for the wheel position, i.e., $e_{1,s} = 0$, we introduce a compensation term β_c in the controller design, and $\beta_c = \tau_s$. The new control law is as

$$u = u_{\text{flc}} + \tau_s. \tag{14}$$

With the compensation term, now, we have $u_{\text{flc},s}$ in (13) equal to zero, and $e_{1,s} = 0$.

V. Implementation and Experimental Results

A. Regulation Task

For implementation, we start with a simple control task that is to balance the robot at the original position on a flat surface, i.e., $x_r = 0$, $v_r = 0$, and $\varphi = 0$.

The feedback gains for the linear controller (8) are obtained through the LQR method. We choose $Q = \{100, 0.1, 900, 1\}$ and $R = 1$ and have $\mathbf{k} = [k_1, k_2, k_3, k_4]^{\text{T}} = [-10.0000, -13.2218, -35.3382, -3.4504]^{\text{T}}$, which generates perfect control performance in simulations, as shown in Fig. 7. The initial states of the 2WMR are as $[x, \dot{x}, \theta, \dot{\theta}]^{\text{T}} = [0, 0, 0.3, 0]^{\text{T}}$. The regulation task is achieved in a fairly short time when the wheels stop at the origin position and the pendulum is stabilized at the upright position. The responses of the wheel position and the pendulum angle are smooth and without steady-state errors.

Considering the existence of mismatch between the real-time system model and the nominal model [(1) and (2)], the feedback gains obtained by simulation need to be adjusted through experimental testings on the 2WMR prototype. In order to find appropriate feedback gains, the linear controller (8) is applied for testing, and strong vibrations are observed. For systems having backlash in the driving mechanism, large feedback gains could easily incur vibrations [5]. In our 2WMR system, the backlash is produced by the gearbox. Since the ultimate control objective is to achieve the position control of the wheels and stabilize the pendulum, large feedback gains are necessarily needed for the position terms; hence, k_1 and k_3 should be kept at the original designed level. Therefore, in order to reduce or avoid vibrations, the feedback gains for the velocity terms k_2 and k_4 should be minimized [5]. From the experimental testing, we observe that the system vibration reduces significantly as k_2 and k_4 decrease. After several trials, the feedback gains are adjusted to $\mathbf{k} = [-10, -0.5, -35, -1.5]^{\text{T}}$.

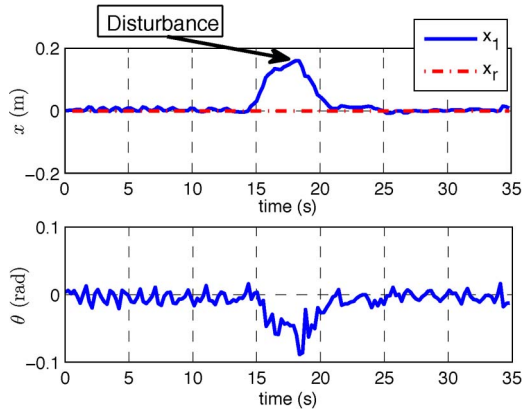

Fig. 8. Experimental testing results for the regulation task: Time responses of x and θ under the FLC proposed in this work. The 2WMR is placed on a flat surface.

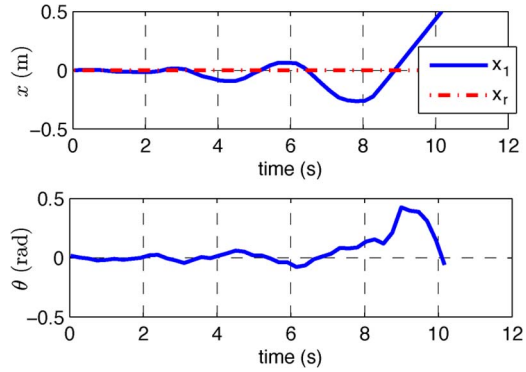

Fig. 9. Experimental testing results for the regulation task: Time responses of x and θ under the linear controller [5]–[8] with feedback gains as $\mathbf{k} = [-10, -0.5, -35, -1.5]^{\text{T}}$. The 2WMR is placed on a flat surface.

Based on the obtained feedback gains, the FLC output parameters are computed in the way introduced in Section IV-B, and we have $[n_1, n_2, n_3, n_4, n_5, n_6, n_7, n_8] = [23.79, 23.44, 13.79, 13.44, 23.19, 22.84, 13.19, 12.84]$. The FLC in (14) is applied with $\tau_s = 0$ and $\theta_r = 0$. The experimental results are shown in Fig. 8. The FLC shows effectiveness that the 2WMR stays around the original position and the pendulum is balanced around $\theta = 0$. At $t = 15$ s, we push the 2WMR to the right about 0.15 m, which can be considered as a disturbance to the system. The 2WMR moves backward and stops at the origin position within 3 s.

For comparison, several existing methods, including the linear controller proposed in [5]–[8], the fuzzy traveling and position controller (FTPC) proposed in [4], and the sliding-mode controller (SMC) proposed in [12] and [13], are used to control the 2WMRs. Fig. 9 shows the experimental results for the 2WMR system under the linear controller with feedback gains as $\mathbf{k} = [-10, -0.5, -35, -1.5]^{\text{T}}$; it can be seen that the system becomes unstable in 10 s. Fig. 10 shows the experimental results for the 2WMR system under the linear controller with feedback gains as $\mathbf{k} = [-20, -1, -70, -3]^{\text{T}}$, which is twice as that used in the preceding testing. The 2WMR is stabilized around the initial position; however, it becomes unstable when a disturbance is added to the system at $t = 20$ s, which indicates the limited robustness of the linear controller. Fig. 11 shows

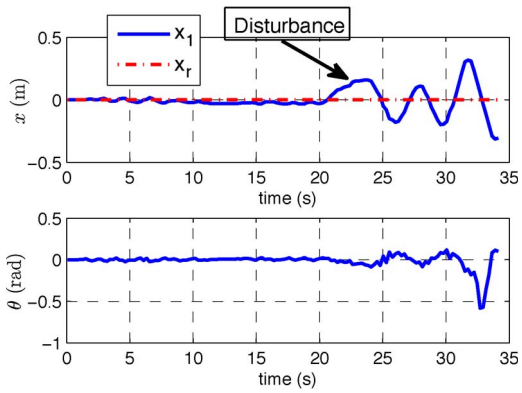

Fig. 10. Experimental testing results for the regulation task: Time responses of x and θ under the linear controller [5]–[8] with feedback gains as $\mathbf{k} = [-20, -1.0, -70, -3]^{\mathrm{T}}$. The 2WMR is placed on a flat surface.

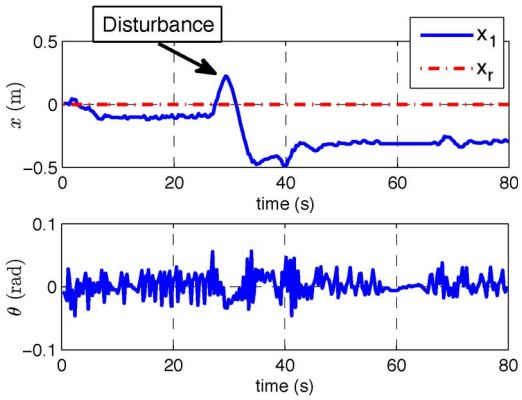

Fig. 11. Experimental testing results for the regulation task: Time responses of x and θ under the FTPC [4]. The 2WMR is placed on a flat surface.

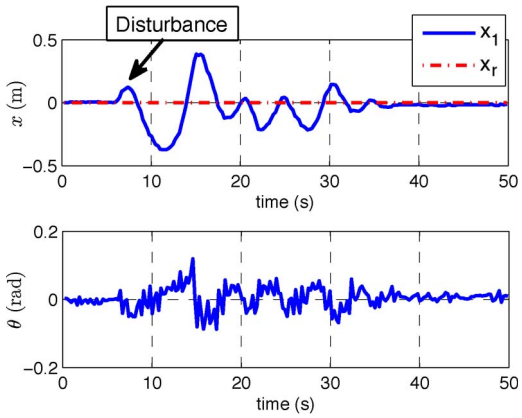

Fig. 12. Experimental testing results for the regulation task: Time responses of x and θ under the SMC [12], [13]. The 2WMR is placed on a flat surface.

the experimental results for the 2WMR system under the FTPC [4]. The pendulum of the 2WMR can be stabilized; however, the wheel position control fails where steady-state errors exist in the wheel position response, which shows the limitation of the FTPC. Fig. 12 shows the experimental results for the 2WMR system under the SMC [12], [13]. The 2WMR is finally stabilized at the initial position even if a disturbance is added to the system at $t = 6$ s. However, the transient response is

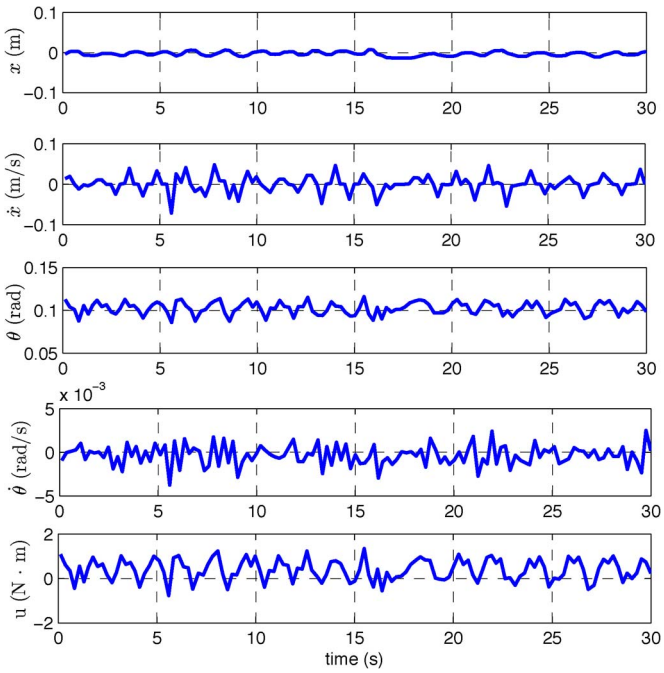

Fig. 13. Experimental testing results for the regulation task: Time responses of x, $\dot{x}$, θ, $\dot{\theta}$, and u under the FLC with $\theta_r = 0.09$ rad and $\tau_s = 0.1855$ N · m. The mobile robot is placed on an inclined surface with $\varphi = 4.3°$.

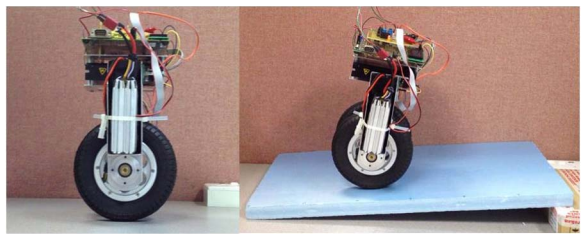

Fig. 14. Images for the regulation task. The 2WMR is balanced on the flat and the inclined surface.

not satisfactory, i.e., the response of the wheel position shows oscillation, and the settling time is around 30 s.

From the experimental results shown in Figs. 8–12, it is evident that the FLC proposed in this work provides a better performance than the existing methods when controlling the 2WMR.

Next, the 2WMR is placed on an inclined surface with the slope angle $\varphi = 4.3°$. According to (11) and (12), we have $\theta_r = 0.09$ rad and $\tau_s = 0.1855$ N · m. The FLC in (14) is applied. Other control parameters are chosen the same as those in the test for regulation on a flat surface. The experimental results are shown in Fig. 13. The FLC shows effectiveness that the 2WMR stays around the original position and the pendulum is balanced around $\theta = 0.1$ rad. It is also observed that the average value of the control signal is positive.

The images of the 2WMR for the regulation task under the FLC are shown in Fig. 14; we can see that the pendulum is balanced at the upright position when it is placed on the flat surface but tilts rightward a bit when it is balanced on the inclined surface. The experimental results are consistent with the theoretical analysis in Section IV-C.

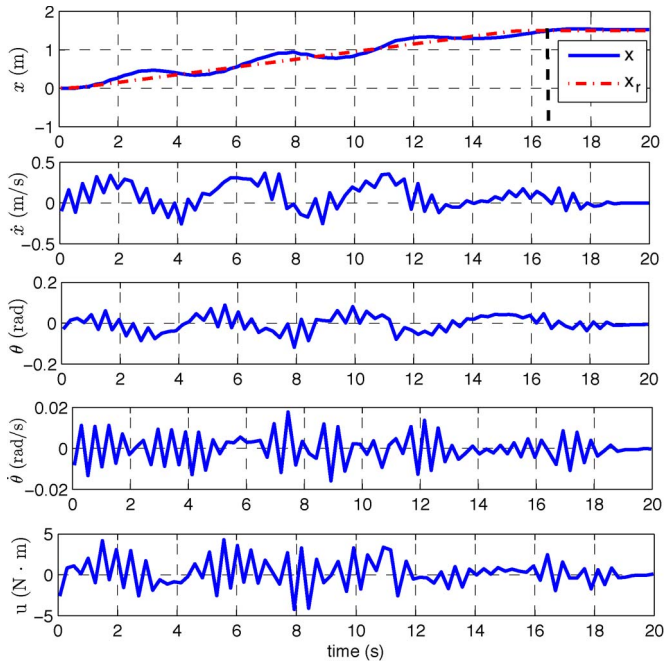

Fig. 15. Experimental testing results for the setpoint control task: Time responses of x, $\dot{x}$, θ, $\dot{\theta}$, and u under the FLC with $\theta_r = 0$ and $\tau_s = 0$. The mobile robot travels on a flat surface. The reference trajectory (4) is applied.

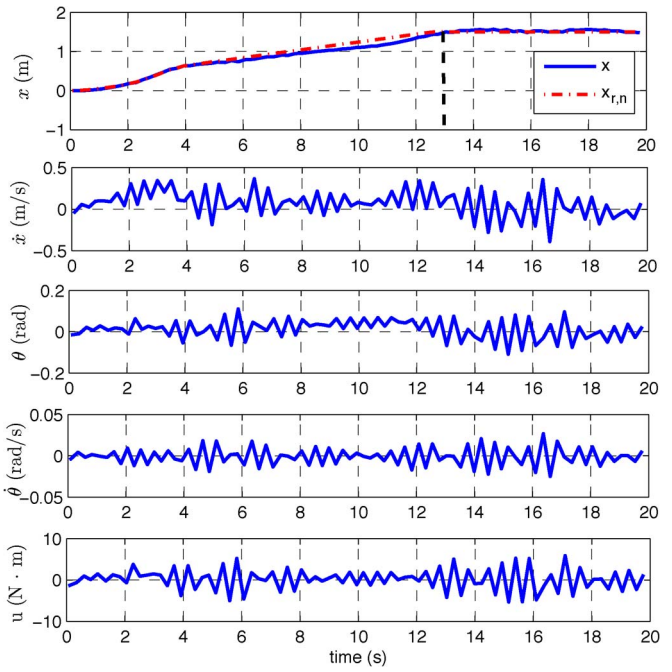

Fig. 16. Experimental testing results for the setpoint control task: Time responses of x, $\dot{x}$, θ, $\dot{\theta}$, and u under the FLC with $\theta_r = 0$ and $\tau_s = 0$. The mobile robot travels on a flat surface. The modified reference trajectory (15) is applied.

B. Setpoint Control Task

First, we consider that the mobile robot travels on a flat surface, i.e., $\varphi = 0$. x_r and v_r in Fig. 3 are used. All controller parameters are chosen the same as those for the regulation task. The experimental results are shown in Fig. 15. The 2WMR reaches the desired setpoint $x_d = 1.5$ m at $t = 16.5$ s and stays there afterward. The FLC shows effectiveness for setpoint control of the 2WMR system. However, the response of the wheel position is not satisfactory because the backward motion exists. When the real position of the 2WMR x_1 surpasses the given reference x_r, the 2WMR would stop for a while or travel backward to make $|x_1 - x_r|$, i.e., $|e_1|$, become smaller, which is natural in a feedback control system. However, considering that our objective for the 2WMR is traveling forward to arrive at the desired position, these motions are not desired.

To improve the 2WMR performance, particularly the response of the wheel position, we propose a modified reference trajectory $x_{r,n}$ for the wheel position as the following:

$$x_{r,n}(t+T_s) = \begin{cases} x_{r,n}(t) + v_r T_s, & \text{if } x_1(t) \le x_{r,n}(t) < x_d \\ x_1(t) + v_r T_s, & \text{if } x_{r,n}(t) < x_1(t) < x_d \\ x_d, & \text{if } x_{r,n}(t) \ge x_d \text{ or } x_1(t) \ge x_d. \end{cases} \quad (15)$$

The idea is to avoid the undesired backward motion. The modified reference trajectory $x_{r,n}$ is adaptive in the sense that it is updated according to the current position of the 2WMR. When the wheel position x_1 surpasses the given reference $x_{r,n}$, we regard x_1 as the new starting point to generate the reference for the next sampling time; thus, the error between the real position of the wheel and the reference $e_1 = x_{r,n}(t + T_s) - x_1(t) = v_r T_s$ is guaranteed to be positive. As a result, the undesired backward motion is avoided, and the 2WMR performance is improved.

Another test is conducted with applying the modified reference trajectory $x_{r,n}$. The FLC parameters are the same as those in the preceding test. The experimental results are shown in Fig. 16. We can see that the 2WMR keeps on moving forward and reaches the desired setpoint $x_d = 1.5$ m at $t = 13$ s. The pendulum is balanced around $\theta = 0$, i.e., the upright position. It is evident that the response of the wheel position in Fig. 16 is much smoother compared with the results shown in Fig. 15, and the 2WMR arrives at the desired position in a shorter time, which shows the effectiveness of the proposed modified reference trajectory $x_{r,n}$.

Next, we consider that the mobile robot travels on an inclined surface with the slope angle $\varphi = 2.45°$. According to (11) and (12), we have $\theta_r = 0.05$ rad and $\tau_s = 0.1$ N · m. To obtain a smooth and fast response, similarly, the reference trajectory in (15) is used. The FLC in (14) is applied. The experimental results are shown in Fig. 17. We can see that the robot travels smoothly and reaches the desired position at $t = 10$ s without steady-state error. The pendulum is balanced around $\theta = 0.05$ rad.

C. Discussions

From the experimental testings, it is found that the designed FLC outperforms the linear controller. For the linear controller with fixed feedback gains, when high gains are applied, the system does not perform well during the traveling, and when low gains are applied, the system could easily become unstable

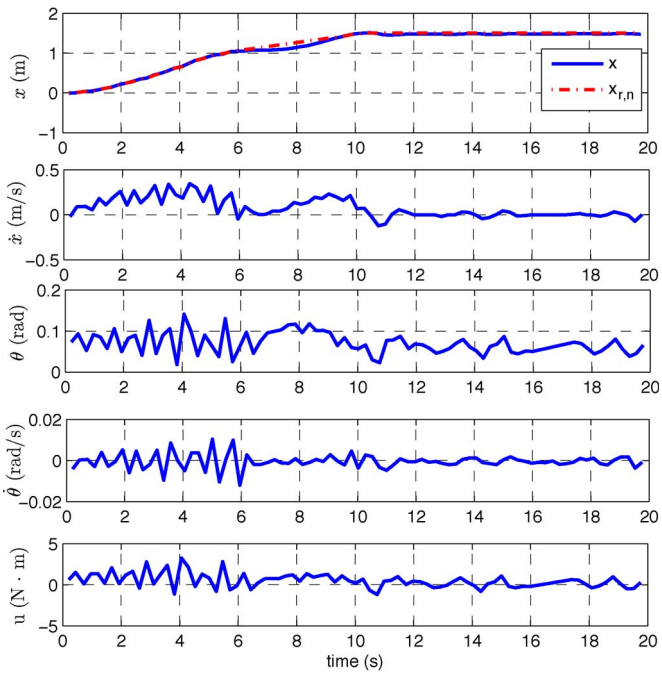

Fig. 17. Experimental testing results for the setpoint control task: Time responses of x, $\dot{x}$, θ, $\dot{\theta}$, and u under the FLC with $\theta_r = 0.05$ rad and $\tau_s = 0.106$ N · m. The mobile robot travels on an inclined surface with $\varphi = 2.5°$. The modified reference trajectory (15) is applied.

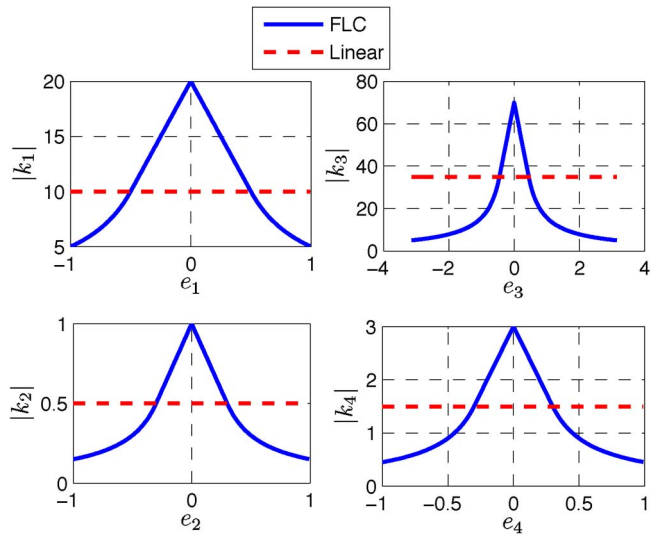

Fig. 18. Comparisons between the fixed feedback gains of a linear controller and the equivalent feedback gains of the FLC.

for the regulation task or after the setpoint is reached. The FLC shows effectiveness for various control tasks under a group of fixed controller parameters. The reason is that the FLC functions as a feedback controller with varying gains, as we stated in Section IV-B. For a clear explanation, we have conducted the following analysis. Fig. 18 shows the comparisons between the fixed feedback gains of a linear controller and the equivalent feedback gains of the FLC, which are computed in the following manner:

$$k_i = \frac{u_{\text{flc}}}{e_i} \text{ at } e_j = 0 \qquad (i, j = 1, 2, 3, 4 \text{ and } j \neq i).$$

For the calculation of k_1, let $(e_2, e_3, e_4) = (0, 0, 0)$; from Fig. 4, we have $[\mu_P(e_j), \mu_N(e_j)] = [0.5, 0.5]$, $j = 2, 3, 4$. It follows that

$$\mu_{R^i} = \begin{cases} \mu_P(e_1) \cdot 0.5^3, & \text{for } i = 1, 2, 5, 6, 9, 10, 13, 14 \\ \mu_N(e_1) \cdot 0.5^3, & \text{for } i = 3, 4, 7, 8, 11, 12, 15, 16. \end{cases}$$

We have

$$k_1(e_1) = \frac{u_{\text{flc}}}{e_1} = \frac{0.125\,[\mu_P(e_1) - \mu_N(e_1)]}{e_1} \sum_{i=1}^{8} n_i. \tag{16}$$

Similarly, we have

$$k_j(e_j) = \frac{u_{\text{flc}}}{e_j} = \frac{0.125\,[\mu_P(e_j) - \mu_N(e_j)]}{e_j} \sum_{i=1}^{8} n_i, \quad j = 2, 3, 4. \tag{17}$$

Since $\sum_{i=1}^{8} n_i$ is a constant, it can be concluded that the equivalent feedback gains of the FLC are determined by the membership functions.

From Fig. 18, we can see that $|k_j|$ drops as e_j increases, which is desirable for the real implementation. When the states of the 2WMR are close to the desired values, i.e., the error states $\mathbf{e}$ are small, the control signal is small. High gains are needed to achieve robustness, considering the fact that the real-time platform is under various uncertainties, such as joint friction, ground friction, backlash, and unmodeled motor dynamics. When the states of the 2WMR are away from the desired values, i.e., the error states $\mathbf{e}$ are large, a group of relatively lower gains are preferred, considering that the motor capacity is limited and the control signal could be saturated if high gains are applied, which would devastate the effectiveness of the feedback controller. The FLC with the selected membership function (5) provides such varying gains that are adapted to the current states of the 2WMR, which indicates the advantage of the selected membership functions and explains that the designed FLC outperforms the linear controller.

VI. Conclusion

In this paper, the synthesized design of a T–S-type FLC for an underactuated 2WMR has been presented. The FLC design is based on both human experience and information of the system dynamic model. The proposed FLC was successfully implemented on a real-time 2WMR, and extensive experimental testings were conducted. For the regulation task, the FLC shows effectiveness that the 2WMR stays around the original position and the pendulum is balanced around the equilibrium position. For the setpoint control task, the FLC shows effectiveness that the 2WMR reaches the desired setpoint and the pendulum is balanced around the equilibrium position. A modified reference trajectory was applied to further improve the performance of the 2WMR during the traveling. The new FLC outperforms a linear controller, even though the FLC output parameters are tuned according to the output of the linear controller at certain operating points. The design procedure indicates that we can

easily extend a linear controller to a nonlinear one like the FLC to achieve better performance.

APPENDIX
LINEARIZED DYNAMIC MODEL OF THE 2WMR SYSTEM

From (1) and (2) and the definition of the error states $\mathbf{e}$, the state-space model of the error dynamics is obtained as

$$\dot{\mathbf{e}} = \mathbf{f}(\mathbf{e}) + \mathbf{g}(\mathbf{e})(u + d_m) + \mathbf{d}_u(\mathbf{e}, t) \tag{18}$$

where $\mathbf{f}(\mathbf{e}) = [e_2, f_1(\mathbf{e}), e_4, f_2(\mathbf{e})]^{\mathrm{T}}$, $\mathbf{g}(\mathbf{e}) = [0, g_1(\mathbf{e}), 0, g_2(\mathbf{e})]^{\mathrm{T}}$, and $\mathbf{d}_u(\mathbf{e}, t) = [0, d_{u1}(\mathbf{e}, t), 0, d_{u2}(\mathbf{e})]^{\mathrm{T}}$, with

$$\begin{aligned}
f_1 &= \frac{m_p l}{ac - b^2}\left[ce_4^2 \sin(e_3 + \theta_r + \varphi) - bg \sin(e_3 + \theta_r)\right] \\
&\quad - \frac{c(m_p + m_w)g \sin\varphi}{ac - b^2} \\
f_2 &= \frac{m_p l}{ac - b^2}\left[-be_4^2 \sin(e_3 + \theta_r + \varphi) + ag \sin(e_3 + \theta_r)\right] \\
&\quad + \frac{b(m_p + m_w)g \sin\varphi}{ac - b^2} \\
g_1 &= \frac{1}{r}\frac{c}{ac - b^2} + \frac{b}{ac - b^2} \\
g_2 &= \frac{1}{r}\frac{-b}{ac - b^2} + \frac{-a}{ac - b^2} \\
d_{u1} &= \frac{-c}{r(ac - b^2)}\tau_{r,w} \\
d_{u2} &= \frac{b}{r(ac - b^2)}\tau_{r,w} \\
d_m &= \tau_{r,m}
\end{aligned}$$

and $b = m_p l \cos(e_3 + \theta_r + \varphi)$.

We linearize the dynamic model of the 2WMR (18) at the desired equilibrium point by assuming that $\sin e_3 \approx e_3$, $e_4^2 \approx 0$, $\cos e_3 \approx 1$, $\tau_{r,m} \approx 0$, $\tau_{r,w} \approx 0$, and φ is known. The linearized dynamic model is

$$\dot{\mathbf{e}} = \underbrace{\begin{bmatrix} 0 & 1 & 0 & 0 \\ 0 & 0 & \frac{-b_0 m_p l g \cos\theta_r}{ac - b_0^2} & 0 \\ 0 & 0 & 0 & 1 \\ 0 & 0 & \frac{am_p l g \cos\theta_r}{ac - b_0^2} & 0 \end{bmatrix}}_{A_0} \mathbf{e} + \underbrace{\begin{bmatrix} 0 \\ g_{1,0} \\ 0 \\ g_{2,0} \end{bmatrix}}_{\mathbf{g}_0} (u + \eta_m) \tag{19}$$

where $\eta_m = -r(m_p + m_w)g \sin\varphi$ and

$$\begin{aligned}
g_{1,0} &= \frac{c}{r\,(ac - b_0^2)} + \frac{b}{ac - b_0^2} \\
g_{2,0} &= \frac{-b_0}{r\,(ac - b_0^2)} + \frac{-a}{ac - b_0^2}
\end{aligned}$$

with $b_0 = m_2 l \cos(\theta_r + \varphi)$.

The term η_m reflects the effect of the gravity when the 2WMR travels on an inclined surface. As we have discussed in Section IV-C, a constant torque τ_s should be provided to overcome the effect of the gravity. It can be seen that η_m is matched to the control input and can be compensated directly by letting $\tau_s = -\eta_m$.

The LQR problem is to minimize the performance index

$$J = \frac{1}{2}\int_0^\infty (\mathbf{e}^{\mathrm{T}} Q \mathbf{e} + u^{\mathrm{T}} R u)dt. \tag{20}$$

The control law is as $u = -\mathbf{k}^{\mathrm{T}}\mathbf{e}$, with $\mathbf{k} = R^{-1}P\mathbf{g}_0$, where P is the solution of the following Riccati equation:

$$PA_0 + A_0^{\mathrm{T}}P - P\mathbf{g}_0 R^{-1}\mathbf{g}_0^{\mathrm{T}}P + Q = 0.$$

REFERENCES

[1] K. Pathak, J. Franch, and S. K. Agrawal, "Velocity and position control of a wheel inverted pendulum by partial feedback linearization," *IEEE Trans. Robot.*, vol. 21, no. 3, pp. 505–513, Jun. 2005.

[2] Z. Li and J. Luo, "Adaptive robust dynamic balance and motion controls of mobile wheeled inverted pendulums," *IEEE Trans. Control Syst. Technol.*, vol. 17, no. 1, pp. 233–241, Jan. 2009.

[3] C.-H. Chiu, Y.-W. Lin, and C.-H. Lin, "Real-time control of a wheeled inverted pendulum based on an intelligent model free controller," *Mechatronics*, vol. 21, no. 3, pp. 523–533, Apr. 2011.

[4] C.-H. Huang, W.-J. Wang, and C.-H. Chiu, "Design and implementation of fuzzy control on a two-wheel inverted pendulum," *IEEE Trans. Ind. Electron.*, vol. 58, no. 7, pp. 2988–3001, Jul. 2011.

[5] T. Takei, R. Imamura, and S. Yuta, "Baggage transportation and navigation by a wheeled inverted pendulum mobile robot," *IEEE Trans. Ind. Electron.*, vol. 56, no. 10, pp. 3985–3994, Oct. 2009.

[6] F. Grasser, A. D'Arrigo, S. Colombi, and A. C. Rufer, "JOE: A mobile, inverted pendulum," *IEEE Trans. Ind. Electron.*, vol. 49, no. 1, pp. 107–114, Feb. 2002.

[7] J. Solis and A. Takanishi, "Development of a wheeled inverted pendulum robot and a pilot experiment with master students," in *Proc. 7th ISMA*, Sharjah, UAE, Apr. 20–22, 2010, pp. 1–6.

[8] P. Oryschuk, A. Salerno, A. M. Al-Husseini, and J. Angeles, "Experimental validation of an underactuated two-wheeled mobile robot," *IEEE/ASME Trans. Mechatronics*, vol. 14, no. 2, pp. 252–257, Apr. 2009.

[9] C.-H. Chiu, "The design and implementation of a wheeled inverted pendulum using an adaptive output recurrent cerebellar model articulation controller," *IEEE Trans. Ind. Electron.*, vol. 57, no. 5, pp. 1814–1822, May 2010.

[10] C.-H. Chiu and C.-C. Chang, "Design and development of Mamdani-like fuzzy control algorithm for a wheeled human-conveyance vehicle control," *IEEE Trans. Ind. Electron.*, vol. 59, no. 12, pp. 4744–4783, Dec. 2012.

[11] C.-C. Tsai, H.-C. Huang, and S.-C. Lin, "Adaptive neural network control of a self-balancing two-wheeled scooter," *IEEE Trans. Ind. Electron.*, vol. 57, no. 4, pp. 1420–1428, Apr. 2010.

[12] M.-S. Park and D. Chwa, "Swing-up and stabilization control of inverted-pendulum systems via coupled sliding-mode control method," *IEEE Trans. Ind. Electron.*, vol. 56, no. 9, pp. 3541–3555, Sep. 2009.

[13] M.-S. Park and D. Chwa, "Orbital stabilization of inverted-pendulum systems via coupled sliding-mode control," *IEEE Trans. Ind. Electron.*, vol. 56, no. 9, pp. 3556–3570, Sep. 2009.

[14] M. Reyhanoglu, A. Schaft, N. H. McClamroch, and I. Kolmanovsky, "Dynamics and control of a class of underactuated mechanical systems," *IEEE Trans. Autom. Control*, vol. 44, no. 9, pp. 1663–1671, Sep. 1999.

[15] Z. Sun, S. S. Ge, and T. H. Lee, "Stabilization of underactuated mechanical systems: A nonregular backstepping approach," *Int. J. Control*, vol. 74, no. 11, pp. 1045–1051, Jan. 2001.

[16] M. W. Spong, "Energy based control of a class of underactuated mechanical systems," in *Proc. IFAC World Congr.*, Jul. 1996, pp. 431–435.

[17] C. A. Ibanez, O. G. Frias, and M. S. Castanon, "Lyapunov-based controller for the inverted pendulum cart system," *Nonlin. Dyn.*, vol. 40, no. 4, pp. 367–374, Jun. 2005.

[18] C. A. Ibanez and O. G. Frias, "Controlling the inverted pendulum by means of a nested saturation function," *Nonlin. Dyn.*, vol. 53, no. 4, pp. 273–280, Sep. 2008.

[19] R. Olfati-Saber, "Nonlinear Control of Underactuated Mechanical Systems With Application to Robotics and Aerospace Vehicles," Ph.D. dissertation, Massachusetts Inst. Technol., Cambridge, MA, Feb., 2001.

[20] M. T. Ravichandran and A. D. Mahindrakar, "Robust stabilization of a class of underactuated mechanical systems using time scaling and Lyapunov redesign," *IEEE Trans. Ind. Electron.*, vol. 58, no. 9, pp. 4299–4313, Sep. 2011.

[21] R. Xu and U. Ozguner, "Sliding mode control of a class of underactuated systems," *Automatica*, vol. 44, no. 1, pp. 233–241, Jan. 2008.
[22] J. Huang, Z.-H. Guan, T. Matsuno, T. Fukuda, and K. Sekiyama, "Sliding-mode velocity control of mobile-wheeled inverted-pendulum systems," *IEEE Trans. Robot.*, vol. 26, no. 4, pp. 750–758, Aug. 2010.
[23] Y.-W. Liang, S.-D. Xu, D.-C. Liaw, and C.-C. Chen, "A study of T–S model-based SMC scheme with application to robot control," *IEEE Trans. Ind. Electron.*, vol. 55, no. 11, pp. 3964–3971, Nov. 2008.
[24] Z. Q. Guo, J.-X. Xu, and T. H. Lee, "A gain-scheduling optimal fuzzy logic controller design for unicycle," in *Proc. IEEE/ASME Int. Conf. AIM*, Jul. 14–17, 2009, pp. 1423–1428.

Jian-Xin Xu (M'92–SM'98–F'12) received the Ph.D. degree from The University of Tokyo, Bunkyo, Japan, in 1989.

In 1991, he joined the National University of Singapore, Singapore, where he is currently a Professor with the Department of Electrical and Computer Engineering. His research interests lie in the fields of learning theory, intelligent control, nonlinear and robust control, robotics, and precision motion control. He has published over 160 journal papers and five books in the field of systems and control.

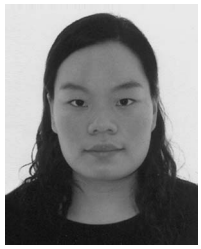

Zhao-Qin Guo received the B.S. degree in control science and engineering from Huazhong University of Science and Technology, Wuhan, China, in 2008. She has been working toward the Ph.D. degree in control science and engineering at the National University of Singapore (NUS), Singapore, since 2008.

Her current research interests include control theories and applications, particularly fuzzy logic control, sliding-mode control, and control of underactuated mechanical systems.

Ms. Guo was a recipient of the NUS Graduate School for Integrative Sciences and Engineering research scholarship in 2008–2012.

Tong Heng Lee received the B.A. degree (with first-class honors) in engineering tripos from the University of Cambridge, Cambridge, U.K., in 1980 and the Ph.D. degree from Yale University, New Haven, CT, in 1987.

He is the Past Vice President for Research of the National University of Singapore, Singapore, where he is currently a Professor with the Department of Electrical and Computer Engineering and also a Professor with the Graduate School for Integrative Sciences and Engineering. He is currently an Associate Editor of *Control Engineering Practice*. He is the Deputy Editor-in-Chief of the IFAC journal *Mechatronics*. His research interests are in the areas of adaptive systems, knowledge-based control, intelligent mechatronics, and computational intelligence.

Dr. Lee is currently an Associate Editor of the IEEE TRANSACTIONS ON SYSTEMS, MAN AND CYBERNETICS and the IEEE TRANSACTIONS ON INDUSTRIAL ELECTRONICS.